

Using low-mass stars as a tool: efforts towards precise models

Achim Weiss¹, Victor Silva Aguirre² and Jørgen Christensen-Dalsgaard²

¹Max-Planck-Institut für Astrophysik, Karl-Schwarzschild-Str. 1, 85748 Garching, Germany
email: aweiss@mpa-garching.mpg.de

²Stellar Astrophysics Centre, Department of Physics and Astronomy, Aarhus University, Ny Munkegade 120, DK-8000 Aarhus C, Denmark

Abstract. We present results of an on-going effort to identify the minimum level of systematic, purely numerical differences in low-mass stellar models on the Red Giant Branch, by comparing models in selected phases for pre-defined physical input assumptions.

Keywords. Stars: interiors, stars: evolution, methods: numerical

1. Introduction

Investigations into the structure and history of galaxies, in particular of the Milky Way, depend primarily on the interpretation of stellar data. To progress from observational data to conclusions about stellar ages, sources of chemical yields, or origin of populations, in almost all cases one depends on stellar models. These may differ appreciably between available model libraries, based on the various stellar evolution codes. One recent example is the determination of stellar parameters in the Kepler LEGACY sample (Silva Aguirre *et al.* 2017), where for a few systems, e.g. the binary system KIC 9139151/163, determined ages differ by 50-100%. While there is a number of reasons for these model-dependent differences, a fundamental question is how relevant the influence of the numerical codes themselves is? (See also Torres *et al.* (2015) or Matson *et al.* (2016).)

In the *Aarhus Red Giant Workshops*, initiated in 2013, and now at its 7th installation, a number of stellar evolution codes have been compared in terms of the resulting models for low-mass red giants, in order to minimize such code differences and to investigate to which level they can be reduced with reasonable effort. The codes participating include *ASTEC* (Christensen-Dalsgaard 2008), *Garstec* (Weiss & Schlattl 2008), *BaSTI* (Pietrinferni *et al.* 2004), *CESAM2k* (Morel & Lebreton 2008), *LPCODE* (Althaus *et al.* 2005), *MONSTAR* (Constantino *et al.* 2014), and *MESA* (Paxton *et al.* 2011, in various versions).

Since we are concerned about the precision of the models, the constituting physics was pre-defined. We have used the NACRE nuclear reaction rates (Angulo *et al.* 1999), the OPAL equation of state (Rogers *et al.* 1996), the OPAL opacities (Iglesias & Rogers 1996), complemented by the Potekhin conductive opacities (Cassisi *et al.* 2007) for the high-density cores of red giants. The solar mixture of Grevesse & Noels (1993) was used. A plane-parallel, grey Eddington atmosphere yields the outer boundary condition. Convection was treated following the mixing-length theory; about the calibration of the parameter α_{MLT} , see below. The effects of overshooting, microscopic diffusion, and mass-loss were ignored, as well as rotation or magnetic fields.

In addition all physical and mathematical constants were checked to be identical. This included values for Newton's constant G and the solar mass M_{\odot} and radius R_{\odot} , since p -mode frequencies of stellar oscillations are very sensitive to the average density and

Table 1. Results of the “solar radius calibration”

Code	ASTECC	CESAM	BASTI	GARSTEC	LPCODE	MESA	MONSTAR
α_{MLT}	2.0438	1.9286	2.0872	1.924	2.072	2.0836	2.047
L/L_{\odot}	1.2032	1.1810	1.2320	1.1866	1.2064	1.2232	1.1869
R/R_{\odot}	1.0000	1.0000	1.0000	0.9986	0.9999	1.0000	1.0001
T_{eff}	6053	6025	6089	6036	6057	6078	6032
X_c	0.2802	0.2951	0.2850	0.2874	0.2903	0.2867	0.2878

are being measured with high precision. For meaningful frequency comparisons between models, GM/R^3 has to be defined within 10^{-4} . Along the sequence of workshops and comparisons more and more additional details of the codes were recognized, which had to be adapted between codes, implying also repeated calculations of the same models. We concentrated so far on masses of 1, 1.5, 2, and $2.5 M_{\odot}$, evolving them from the main sequence to the ignition of helium and into core helium burning.

2. Solar radius calibration

To calibrate the mixing-length parameter α_{MLT} , we fixed the “solar composition” to $X = 0.70$ and $Z/X = 0.0245$ (Grevesse & Noels 1993), and required that at the solar age all codes match the solar radius (but obviously not the solar luminosity). As the implementation of MLT in the various codes differs, the resulting values for α_{MLT} do so as well. They are summarized in Table 1, but notice that also other solar quantities (L , X_c) differ between 1 and 4%, which is surprising, given the simplicity of the Sun and the pre-defined physical input.

We then computed different stellar models with a generic composition of $X = 0.70$, $Z = 0.02$, and compared their properties at specific stellar radii on the RGB. In Fig. 1 (left panel) we show the initial comparison of ages for $2 M_{\odot}$ models, before looking deeper into the codes and adjusting them. The average uncertainty a user of such models has to expect is of order 2%, but outliers (here: 5%) cannot be excluded. The age difference results from the evolution on the main sequence. There, uncertainties are more serious for stars with convective cores. After adjustments outliers (also for other mass values) could be removed, and the overall numerical systematic effect reduced to 1% for the $1 M_{\odot}$ model. Interestingly, the remaining age differences are larger on the main sequence, which most likely relates to slightly different core sizes, and which is reduced on the RGB, once the He-core grows larger than the core on the MS, indicating a consistent mass-energy conversion in all codes. For the $1.5 M_{\odot}$ models, however, two codes produced models, which differed from all others by up to 10% in age in all evolutionary phases. This is connected to the treatment of a growing convective core on the MS (see Gabriel *et al.* 2014, for the difficulties connected with this situation). In the right panel of the same figure the tracks in the HRD for $1 M_{\odot}$ models around the RGB-bump are displayed (after code adjustments). In spite of the α_{MLT} calibration the tracks differ here by up to 50 K, and the bump position also varies by a few solar luminosities, indicative of different extensions of the convective envelope. We also found variations in the internal chemical profiles and core masses, but below the 2% level.

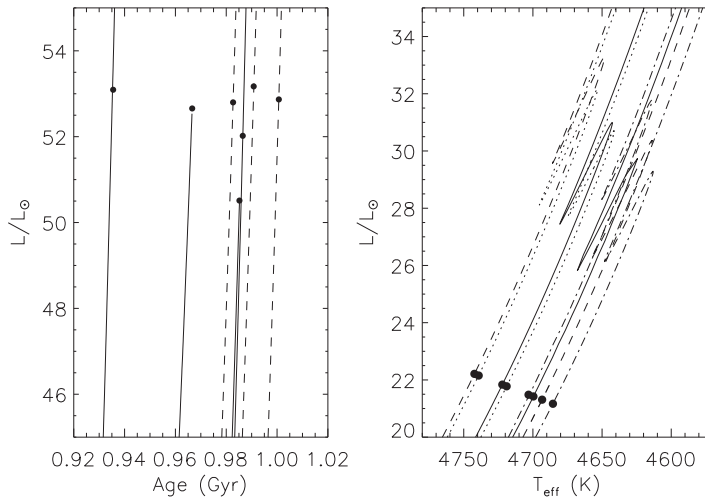


Figure 1. Left: Comparison of ages of stars with $2 M_{\odot}$, showing the initial spread before further code modifications. Notice that the three dashed tracks are all MESA-models, resulting from different code versions and users. The solar values listed in Table 1 are from the central one of these three models. The filled circles indicate models with $R = 10 R_{\odot}$. Right: The HRD around the RGB-bump, for the various models with $1 M_{\odot}$. Filled circles indicate the comparison target of $R = 7 R_{\odot}$.

3. α_{MLT} -calibration on the RGB

In order to avoid the T_{eff} -differences on the RGB, which result, for given radius, in different luminosities, and thus, due to the core mass – luminosity – relation in different core sizes, we calibrated α_{MLT} in a second exercise on the RGB, such that all models matched T_{eff} of one reference model. Consequently, T_{eff} differed on the MS by up to 100 K \dagger , but core sizes and chemical profiles on the RGB agreed within the 1% level.

As before, the presence of convective cores deteriorates the agreement of models. This is exemplified in Fig. 2 for the $2 M_{\odot}$ models, where age differences partially exceeded the 5% level, both on the MS and on the RGB, at $10 R_{\odot}$.

4. Other concerns

Since this project originated from seismology needs, we compared the seismic properties of our models, which depend significantly on chemical profiles and the Brunt-Väisälä frequency. In spite of the relatively good agreement of profiles, the BV-frequency differs on the 10% level easily. This has severe consequences for matching models to observed stars with known seismic properties. We are currently investigating the reasons for this.

One issue we identified is the transition between radiative and conductive opacities at higher densities and temperatures. While the opacity sources are the same in all codes, the treatment of the transition for those densities where one of the sources lacks data is different from code to code. It appears that localized differences in $\log \kappa$ of up to 40% are possible, propagating into structure differences. A well-defined transition method is to be developed in future workshops.

\dagger We stress that age determinations based on or relying on T_{eff} are highly uncertain and can easily lead to ages wrong by 25-30%, solely due to model uncertainties.

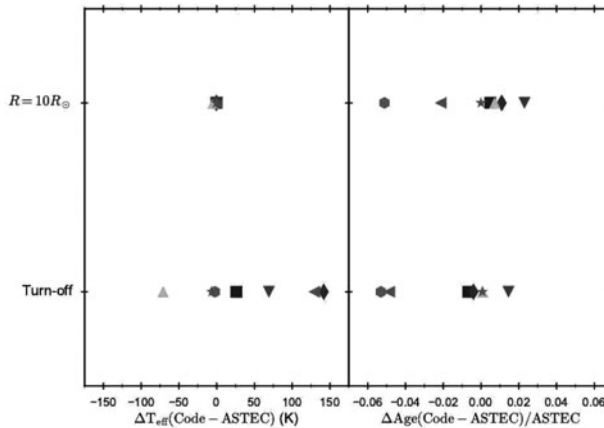


Figure 2. Models for a $2 M_{\odot}$ star, compared at the main sequence turn-off and at a radius of $10 R_{\odot}$. Left: T_{eff} , relative to the *ASTEC* model; right: age, relative to the same reference model.

5. Outlook and summary

We are extending our efforts into the clump phase, i.e. the core helium burning phase. As this includes the core helium flash, additional numerical issues appear for the different codes, some of them not able to follow the flash completely. Also, it is not trivial to define a comparison quantity (core mass, radius, central helium content) in the clump phase, at which to compare models reasonably. We intend to start calculations for all codes from one reference clump model to avoid all differences from previous evolutionary phases.

So far, our conclusion is that the numerical uncertainties can, with some effort, be reduced such that systematic differences in the models are lowered to the few per cent level, in terms of evolutionary and structural properties. We found that all codes had to be scrutinized for lurking problems, but that the effort is worth doing so. An extended report about this project is currently being prepared (Silva Aguirre *et al.*, 2018).

References

- Althaus, L. G., Serenelli, A. M., Panei, J. A., *et al.* 2005, *A&A*, 435, 631
 Angulo, C., Arnould, M., Rayet, M., *et al.* 1999, *Nuclear Physics A*, 656, 3
 Cassisi, S., Potekhin, A. Y., Pietrinferni, A., Catelan, M., & Salaris, M. 2007, *ApJ*, 661, 1094
 Christensen-Dalsgaard, J. 2008, *Ap&SS*, 316, 113
 Constantino, T., Campbell, S., Gil-Pons, P., & Lattanzio, J. 2014, *ApJ*, 784, 56
 Gabriel, M., Noels, A., Montalbán, J., & Miglio, A. 2014, *A&A*, 569, A63
 Garcia, E. V., Stassun, K. G., Pavlovski, K., *et al.* 2014, *Astron. J.*, 148, 39
 Grevesse, N. & Noels, A. 1993, in 35ème cours de perfectionnement de l'Association Vandoise des Chercheurs en Physique, eds. B. Hauck, S. Paltani, & D. Raboud (AVCP, Lausanne), 205
 Iglesias, C. A. & Rogers, F. J. 1996, *ApJ*, 464, 943
 Matson, R. A., Gies, D. R., Guo, Z., & Orosz, J. A. 2016, *Astron. J.*, 151, 139
 Morel, P. & Lebreton, Y. 2008, *Ap&SS*, 316, 61
 Paxton, B., Bildsten, L., Dotter, A., *et al.* 2011, *ApJS*, 192, 3
 Pietrinferni, A., Cassisi, S., Salaris, M., & Castelli, F. 2004, *ApJ*, 612, 168
 Rogers, F. J., Swenson, F. J., & Iglesias, C. A. 1996, *ApJ*, 456, 902
 Silva Aguirre, V., Lund, M. N., Antia, H. M., *et al.* 2017, *Astrophys. J.*, 835, 173
 Torres, G., Claret, A., Pavlovski, K., & Dotter, A. 2015, *Astrophys. J.*, 807, 26
 Weiss, A. & Schlattl, H. 2008, *Ap&SS*, 316, 99